
Modeling the Temperature and Ice-Thickness Profiles Within OMEGA Cryogenic Targets

Introduction

Cryogenic targets for direct-drive experiments on OMEGA require a 100- μm -thick layer of solid hydrogen isotopes (DT or D_2) uniformly distributed around the inside of a thin-walled (1 μm), 1-mm-diam polymer capsule. This uniformity is achieved by maintaining the capsule in a uniform and stable thermal environment where the inner and outer ice surfaces are each positioned along a single isotherm. The hydrogen fuel is layered¹⁻³ in the following sequence: the capsule is permeation-filled with gaseous DT or D_2 ; the gas is cooled to the liquid phase, then gradually cooled through the triple point; polycrystalline DT or D_2 solid expands from a single nucleation site. Heat provided during cooling through the triple point is needed to sublime the hydrogen ice from regions where the ice is thickest and redeposit it where ice is thinnest to form a uniformly thick layer. For solid DT this energy is provided by the radioactive decay of a triton atom, which produces an electron with a mean energy of 4.6 keV and provides 12 μW of uniform bulk heating in an OMEGA target. D_2 layers require an external source of heat, which is provided by an IR light source operating at the strongest vibrational-rotational absorption frequency of the D_2 lattice (3.2 cm^{-1}).

The allowed deviation of the inner ice layer from a completely smooth symmetrical geometry is less than 1- μm rms for all spherical Legendre modes $\ell < 50$.⁴ This demanding specification requires a diagnostic technique that is capable of measuring how accurately the capsule is positioned along the isotherms within the layering sphere. The only available technique with the requisite sensitivity is the interferometric technique used to measure the smoothness of the ice layer.⁵ The uniformity and smoothness of the ice are the best measures of the thermal environment in the layering sphere. Since the interferometric technique is also in development, additional information is needed to understand the thermal environment present in the layering sphere to allow us to iterate the layering and characterizing development process. This information can be obtained only by numerical simulation and is needed to define the initial layering conditions. As experimental data becomes available, the theoretical model can be refined.

This work is an initial endeavor to develop a numerical model of the thermal conditions of a cryogenic target inside the layering sphere. The layering sphere is a spherical cavity containing two sets of orthogonal windows for viewing and a hole for inserting and removing the target. The temperature gradients within the ice are calculated for specific conditions and nonuniformities inside the layering sphere. This allows the pressure inside the capsule and the ice thickness to be calculated from the measurable temperature on the layering sphere. The numerical simulations are validated against analytic solutions where possible. The sensitivity of the ice layer's uniformity to the effects of three principal nonuniformities are calculated: (1) misalignment of the capsule from the center of the layering sphere; (2) variability in the uniformity of the capsule wall thickness; and (3) temperature gradients on the internal surface of the layering sphere. Knowing the magnitude of these effects will guide our target fabrication and cryo-engineering research priorities.

A commercially available computational fluid dynamics (CFD) code *FLUENT*⁶ is used to model the cryogenic target in the layering sphere. This code employs an advanced variable-size mesh generation mechanism that provides maximum computational resolution where it is most needed. *FLUENT* also possesses two properties that are required for more sophisticated modeling: (1) it allows mass transport to be calculated concurrently with thermal calculations, and (2) it has the provision to model condensation, an integral component of the layering process.

Two-dimensional (2-D) axisymmetric models of the environment, which included the layering sphere, exchange gas, target capsule, and DT-ice layer, were used for the calculations. The models were created with *GAMBIT* (Fluent, Inc.) geometry/mesh generation software, the companion program to *FLUENT*. For these initial calculations, the target mount, layering sphere windows, and target-extraction hole were not included in the models. The geometry of the environment, along with the meshing scheme, is shown in Figs. 81.11 and 81.12. A finer mesh was used in the ice and capsule, where

greater temperature resolution was required, while a gradually coarser mesh was used in the exchange gas extending to the layering sphere's inside surface. The cell size in the ice was $10 \times 10 \mu\text{m}^2$, and the complete environment totaled over 15,000 cells.

The layering sphere had an inside diameter of 25.4 mm. The capsule, which was centered in the layering sphere (unless decentered for modeling purposes), had an outside diameter of $950 \mu\text{m}$ and a wall thickness of $2 \mu\text{m}$. The DT ice was a $100\text{-}\mu\text{m}$ -thick layer on the inside of the capsule. The geometry was considered symmetric about the vertical axis; therefore, only half the overall geometry was modeled. A 50-mTorr helium exchange gas was placed in the layering sphere to allow heat conduction between the target and the layering sphere.

With this model the dimensions (thickness) of the capsule and ice could be readily changed, simulating capsule non-uniformities and DT layering, respectively. Also, the target's position within the layering sphere could be changed easily. This flexibility allowed many situations to be modeled, and the steady-state ice-thickness profile was calculated iteratively.

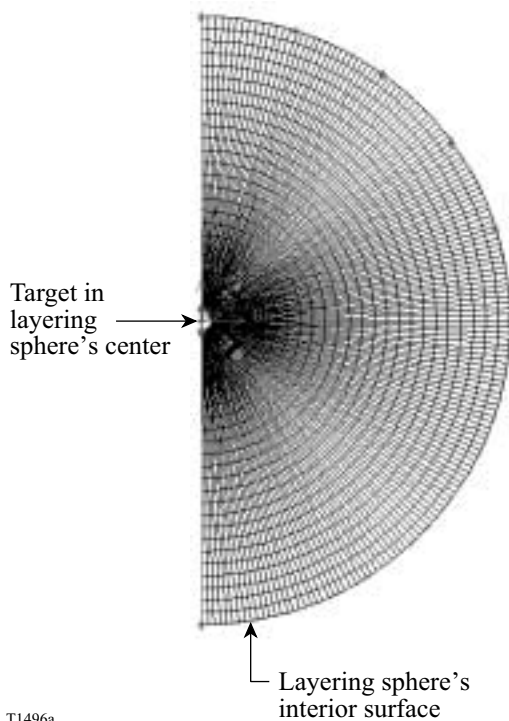


Figure 81.11
Axisymmetric 2-D geometry/mesh of the target capsule, DT ice, helium exchange gas, and layering sphere's interior surface used in the CFD simulation. The inside diameter of the layering sphere is 25.4 mm, and the outside diameter of the capsule is $950 \mu\text{m}$.

The temperature-dependent properties of the materials in the model were used at 18.5 to 20 K whenever possible. The properties of the capsule material—polyimide (Kapton)—were taken from literature and product specifications supplied from DuPont. These are listed in Table 81.I.

To first order, a uniform and stable thermal environment will produce a uniform hydrogen fuel layer if a perfectly spherical capsule with a uniformly thick wall is positioned at the center of an isothermal layering sphere. In actual operation, deviations from ideality exist, which will affect the uniformity of the ice. The following three models were generated to calculate the magnitude of these deviations from ideality on the steady-state temperature and ice-thickness profiles.

Case 1: Misalignment of the Target from the Center of the Layering Sphere.

The target can be moved within the layering sphere using a four-axis motion controller (x, y, z, θ) with an absolute encoder defining its position. The primary goal is to make fine adjustments to position the target at the center of the target chamber for the implosion. Generically, it is known that centering the

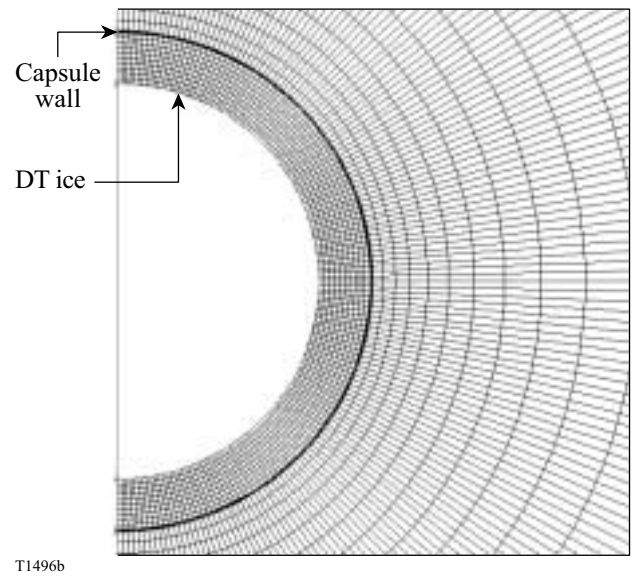


Figure 81.12
Close-up view of the geometry/mesh of the capsule and DT ice used in the CFD simulation. The DT ice is $100 \mu\text{m}$ thick, and the capsule is $2 \mu\text{m}$ thick.

Table 81.I: Properties of the materials used in the CFD simulation.

	Solid DT ⁷	Polyimide (Kapton) ^{8,9}	Helium at 50 mTorr ¹⁰
Thermal conductivity k (W/m K)	0.35	0.05	0.0227
Heat capacity C_p (J/kg K)	2720	130	5600
Density ρ (kg/m ³)	257.6	1500	0.0002
Heat-generation rate Q (W/m ³)	51000	0	0

uniform target in the layering sphere is critical to achieve a uniform ice layer; however, the sensitivity of the target’s position in the uniformity layering sphere to the ice is not known. When the center of the target does not coincide with the center of the layering sphere, the side of the capsule farthest from the layering sphere’s surface will be warmer than the side closest to the layering sphere. (The cooler walls of the layering sphere act as a heat sink for the heat-generating target.) This results in a nonisothermal inner-ice-surface temperature and a consequent thinning of the ice from the warmer side. At steady-state conditions an ice-thickness nonuniformity is created.

Case 2: Capsule-Wall-Thickness Nonuniformities.

Direct-drive target capsules have been produced with a high degree of uniformity in dimension and thickness.¹¹ The current method of measuring the variability in the wall thickness is white-light interferometry and has an accuracy of one interferometric fringe $\sim 0.3 \mu\text{m}$. This case studies the effect of a capsule nonuniformity, which is too small to be measured, on the ice thickness. (If it is found to be significant, a more accurate method will have to be used to select quality capsules.) These nonuniformities in the capsule wall can lead to thermal gradients in the ice as thinner areas in the wall offer less thermal resistance to heat loss to the exchange gas than do thick ones. As research continues on engineering precise uniform capsules, the effects that nonuniformly thick capsules have on cryogenic layers must be calculated.

Case 3: Temperature Gradients on the Inner Surface of the Layering Sphere.

During calculations for Cases 1 and 2, it was assumed that the layering sphere was isothermal; that premise will be investigated here. In this case, the effects that a temperature nonuniformity over 12% of the layering sphere’s inner surface will produce in the target at the center of the layering sphere were calculated. The source of the heat load could be (1) a localized, small thermal short to an adjacent shroud along an instrumentation sensor or the optical fiber used for IR layering and/or

(2) heating on the windows during IR layering and target viewing, and from external radiation. Depending on the magnitude of the temperature nonuniformity, polar and azimuthal temperature gradients may develop in the ice. The effects of these heat sources must be identified by calculations so they can be minimized by engineering.

The most obvious initial concern—heating caused by room-temperature radiation—is not expected to be a significant contributing factor: radiation will be absorbed in the windows (BK glass) of the first stage of the cryocooler, which are at 45 K. Less than 0.4% of the light is transmitted by these 1-mm-thick glass windows. (Re-radiation from these windows at 45 K through the layering sphere’s sapphire windows was calculated to heat the target by less than 20 nW, which is negligible.)

The Target Viewing System (TVS) is used to illuminate and view the target when it is positioned in the center of the target chamber. Absorption of this radiation in the sapphire windows is a contributor to a nonuniform layering-sphere temperature. The source is filtered to 532 nm with a bandwidth of 40 nm, and the heat load is localized around the windows. Because of the excellent thermal conductivity of the copper layering sphere, that area is expected to have a temperature nonuniformity of the order of 1 mK. (If the illumination source is unfiltered, the heat absorbed in the sapphire window is $\sim 40 \text{ mW}$.)

A nonisothermal layering-sphere surface will transmit its effects into the surrounding helium exchange gas, which will produce an uneven heat load on the capsule. The nonuniform capsule environment will result in a shift in the target isotherms to create a nonuniform cryogenic-fuel layer.

Solution Procedure

Separate models were developed to determine the sensitivity of the smoothness of the DT ice to deviations from ideal boundary conditions that may be expected in actual operations. This was done to identify those parameters that most affected

the layer's smoothness. Only heat transfer via conduction was modeled: the pressure of the helium exchange gas (50 mTorr) is too low for convection to contribute to heat flow, and the small temperature gradients between the capsule and the layering sphere preclude a significant radiation effect. (A more complicated refinement to be added later will incorporate mass transfer and the presence of helium inside the capsule into the model. This will allow the dynamics and time dependency of the layering process to be determined. These capabilities will be needed to complement the experimental observations.)

An iterative procedure was used to calculate the final ice profile. Initially, the ice was defined as a uniformly thick layer inside the capsule to calculate the heat generation and the temperature gradient over the ice thickness. Next, a new boundary condition was established to introduce a perturbation of interest, and the resultant temperature profile in the ice was calculated. The ice's void was offset, with the void remaining spherical, to alter the ice thickness and to simulate the layering process. (The solid, which has a temperature-dependent vapor pressure, sublimates and diffuses from the warmer surfaces to the colder surfaces, where it condenses). The simulation was repeated with the adjusted ice geometry, and new temperature profiles were calculated. The process was repeated until the temperature difference on the internal surface of the ice was minimized. At this approximately uniform ice temperature the net transfer of DT would be approximately zero. This convergent configuration was the best approximation of the steady-state ice profile that can be achieved with a spherical void for the prescribed boundary condition.

Results and Discussion

1. Analytical Solutions

An initial, idealized model was created to determine the temperature profile of a uniform spherical ice layer. This model was used for two reasons: (1) to determine the thermal parameter space expected inside the target layering sphere, and (2) to compare the numerical solution to the analytical result to ensure the model was functioning correctly. The model consisted of a uniform 100- μm DT-ice layer inside a 2- μm -thick polyimide capsule with the temperature of the outer layer of the ice constant at 19.5 K (the defined boundary condition). The DT was self-heated with a volumetric heating rate of 51,000 W/m^3 (about 12 μW per target). The numerical simulation calculated the steady-state inner ice temperature to be 19.50065 K. Thus, a radial temperature difference of 650 μK existed between the inner and outer ice surfaces. The temperature profile is shown in Fig. 81.13. This result compared well with the following analytical result.

The steady-state governing equation¹² of a spherical shell with heat generation is

$$\frac{1}{r} \frac{d^2}{dr^2}(rT) + \frac{Q}{k} = 0, \quad (1)$$

where r is the radius, T is the temperature, Q is the heat generation, and k is the thermal conductivity. The boundary conditions are (1) the inner surface, $r = R_i$, is at T_i and the outer surface, $r = R_o$ is at T_o ; (2) no heat transfers from the solid to the gas (assuming negligible thermal conductivity and heat generation in the gas). The solution is given by

$$T_i - T_o = \frac{1}{6} \frac{Q}{k} \left[R_o^2 - R_i^2 - 2R_i^3 \left(\frac{1}{R_i} - \frac{1}{R_o} \right) \right]. \quad (2)$$

This calculation assumes spherical symmetry, i.e., uniform ice thickness and heat transfer solely in the radial direction. Using the dimensions of the ice, $R_o = 473 \mu\text{m}$ and $R_i = 373 \mu\text{m}$, and the thermal conductivity $k = 0.35 \text{ W}/\text{m K}$, the temperature difference between the inner and outer surfaces ($T_i - T_o$) was 630 μK . This result agrees within 3% of the numerical solution, validating the mesh resolution and sensitivity of the numerical approach.

A second model was created to determine the temperature profiles from pole to pole along the outside surface of a nonuniformly thick DT-ice layer. If the ice is uniform, there is no pole-to-pole temperature difference because the heat load is

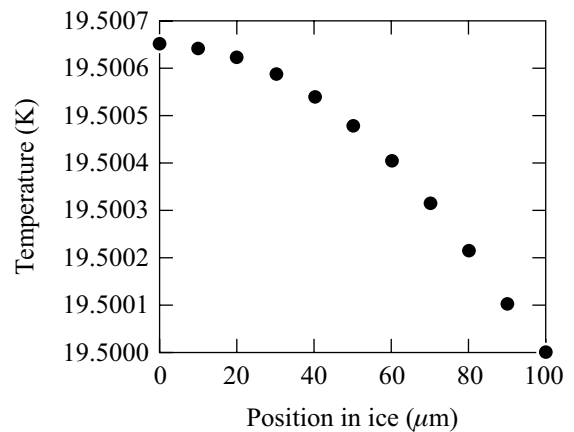


Figure 81.13 Radial temperature profile of a uniformly 100- μm -thick DT-ice layer inside an OMEGA cryo target. The outside ice surface was fixed at 19.5 K. The volumetric heating rate of DT was 51,000 W/m^3 .

symmetric. When thickness variations exist, heat can flow in the tangential direction, leading to a nonisothermal inner ice surface. To model nonuniformities, a 100- μm -thick ice layer was constructed with a 2.0- μm $\ell = 1$ nonuniformity. The model with dimensions is shown in Fig. 81.14. The isothermal boundary condition on the inner surface of the ice was 19.5 K, with all other thermal and material properties of DT the same as the previous model. The CFD simulation predicted a temperature difference ($\Delta T_o = 12 \mu\text{K}$) along the outer surface of the ice.

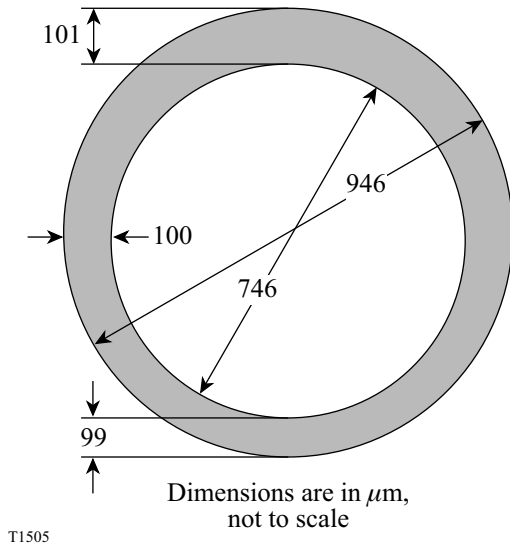


Figure 81.14
A nominal 100- μm -thick ice layer with 2- μm $\ell = 1$ nonuniformity used in the CFD simulation to determine the pole-to-pole temperature difference in nonuniformly thick DT ice.

For the analytical solution, Eq. (2) was rearranged and two calculations were performed. Each calculation gave the temperature of the outer ice surface for a given thickness. The equations were solved by using the inner-surface boundary condition:

$$T_i = \frac{1}{6} \frac{Q}{k} \left[R_o^2 - R_{i1}^2 - 2R_{i1}^3 \left(\frac{1}{R_{i1}} - \frac{1}{R_o} \right) \right] + T_{o1}$$

$$= \frac{1}{6} \frac{Q}{k} \left[R_o^2 - R_{i2}^2 - 2R_{i2}^3 \left(\frac{1}{R_{i2}} - \frac{1}{R_o} \right) \right] + T_{o2}, \quad (3)$$

where the indices “1” and “2” on the radii and temperatures indicate two different locations. By solving the equations with

real radii and properties (shown in Fig. 81.14) and allowing the indices 1 and 2 to refer to the north and south poles, respectively, the temperature difference along the outer ice surface ($\Delta T_o = T_{o1} - T_{o2}$) was 14 μK . This result agrees within 17% of the numerical solution above.

2. Numerical Simulations

The two models above determined the thermal parameter space and compared well with the analytical solutions. The next task was to calculate the effects of realistic perturbations to the system on the DT-ice temperature and thickness profiles. For these more complicated situations, no simple analytical solution existed against which to compare; instead, the numerical models were used to predict the profiles.

Case 1: Misalignment of the target from the center of the layering sphere.

In this model the target was shifted from the center of the layering sphere as shown in Fig. 81.15. The figure depicts the centers of the target and layering sphere offset by 1 mm, about one target diameter. The interior surface of the layering sphere is isothermal at 19.2 K (the prescribed boundary condition). The capsule and DT ice were initially uniform 2 μm and 100 μm thick, respectively. The calculated temperature profiles in the DT ice and vapor space prior to layering are shown in Fig. 81.16. Since the bottom of the target was farthest away from the colder layering sphere, it had the relatively warmer inner ice surface. The pole-to-pole temperature difference along the inner ice surface caused by the target misalignment of 1 mm was 85.5 μK .

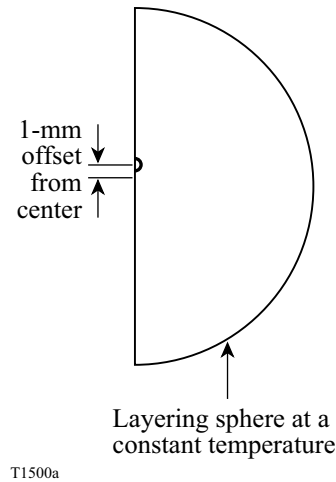


Figure 81.15
Axisymmetric model of a target offset from the center of the layering sphere.

The next step of the simulation was to determine the expected shift in ice thickness caused by the temperature difference on the inner surface. Since the bottom part of the target was warmer, the temperature-dependent vapor pressure of DT above the ice was greater than where the ice was colder. The resulting pressure gradient would create a net mass transfer of DT to the colder, upper half of the target where it condenses on the ice surface. This reduces the ice thickness at the bottom of the capsule and increases it at the top. The semi-circle that represented the inner ice surface was shifted downward to represent the thinning of the lower layer and thickening of the upper layer of DT. Following the iterative solution procedure described previously, the ice's void was manually varied to simulate layering, and the simulation was repeated until the pole-to-pole temperature difference along the ice surface was approximately zero. This occurred when the total ice $\ell = 1$ nonuniformity was $1.1 \mu\text{m}$. (The ice thicknesses at the north and south poles were $100.55 \mu\text{m}$ and $99.45 \mu\text{m}$, respectively.)

The simulation was repeated for different values of the misalignment of the target from the layering sphere's center. The inner ice pole-to-pole temperature differences before redistribution caused by different target offsets are listed in Table 81.II. The corresponding $\ell = 1$ nonuniformities in the DT layer resulting from the offsets are displayed in Fig. 81.17. Using the $\ell = 1$ mode for these analyses is a reasonable compromise as it is the dominant contribution to the total rms roughness⁴ and makes the calculation tractable. Clearly, in actual operation the change in ice thickness would be observed in additional modes of the power spectrum ($\ell > 1$); however, at

present, modeling these additional modes is beyond the scope of this article.

Case 2: Capsule $\ell = 1$ nonuniformities.

The capsule itself can produce temperature nonuniformities in the ice if the wall is not uniformly thick because the capsule's thermal conductivity is much less than that of the ice. The effects of these small perturbations required an adaption to the model. To model the sensitivity of nonuniformities of the order of tenths of microns, the scale of the area under investigation was reduced to include only the target capsule and the DT ice and vapor space. This removed the exchange gas and layering sphere from the calculations. Instead, an isothermal boundary condition on the outer capsule surface at a temperature of 19.5 K was used in all simulations.

Table 81.II: Pole-to-pole temperature difference on the inner DT-ice layer before redistribution for various offsets of the target from the center of the layering sphere.

Offset from center (μm)	Temperature difference in ice (μK)
0	0.0
500	-52.0
1000	-85.5
1500	-190.0

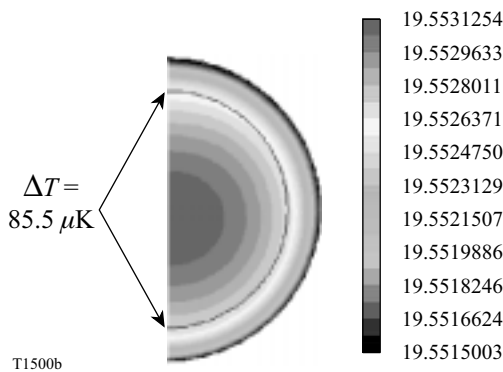


Figure 81.16 Temperature profiles in the DT ice and vapor space for a target offset from the center of the layering sphere by 1 mm. The pole-to-pole temperature difference on the inner ice surface was $85.5 \mu\text{K}$.

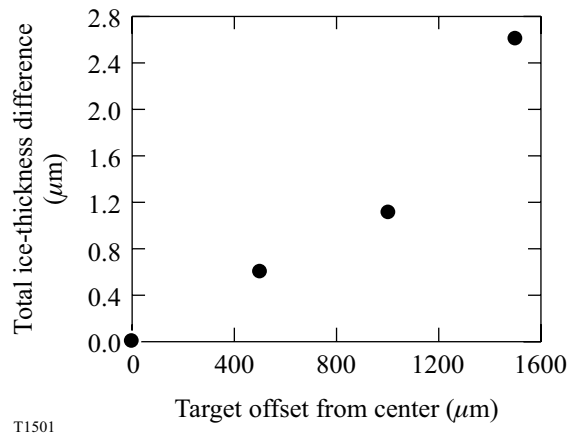


Figure 81.17 Total ice $\ell = 1$ nonuniformity in a nominal $100\text{-}\mu\text{m}$ -thick ice layer for various offsets of the target from the center of the layering sphere.

An example case is shown in Figs. 81.18–81.20. The capsule (nominal thickness $2\ \mu\text{m}$) was modeled to be nonuniform by shifting the semicircle representing the outer shell surface upward by $0.15\ \mu\text{m}$ to create a total $\ell = 1$ nonuniformity of $0.3\ \mu\text{m}$. A uniform $100\text{-}\mu\text{m}$ DT-ice layer was placed inside the nonuniform capsule; the complete geometry is shown in Fig. 81.18. Since there was a greater thermal resistance at the north pole than the south pole due to the thicker capsule wall,

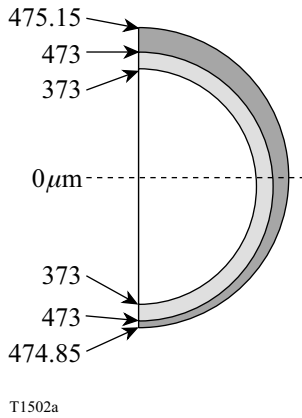


Figure 81.18
A $0.3\text{-}\mu\text{m}$ nonuniformity ($\ell = 1$) in the target-capsule thickness. The ice was $100\ \mu\text{m}$ thick. Figures are not to scale.

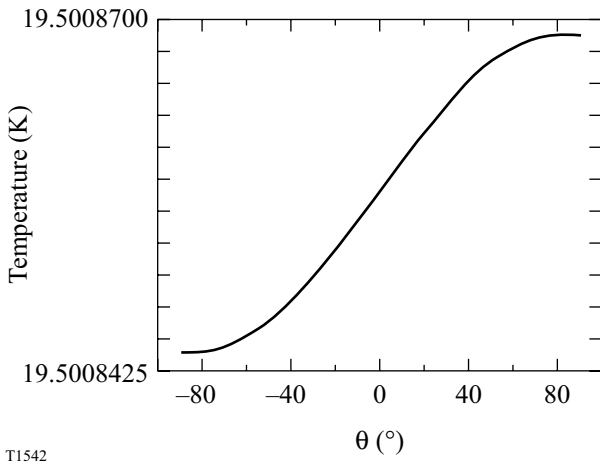


Figure 81.19
Temperature distribution along the inner surface of the ice (0° at target equator, 90° at north pole, -90° at south pole). A pole-to-pole temperature difference occurs as a result of the $\ell = 1$ nonuniformity (capsule thickness nonuniformity).

the ice was relatively warmer at the north pole. The calculated pole-to-pole temperature variation ($\sim 25\ \mu\text{K}$) along the inner ice surface is shown in Fig. 81.19. Using the iterative solution procedure, the ice thickness was shifted to simulate layering (by moving the ice’s free surface) until the temperature gradient between the poles reached zero. This result is shown in Fig. 81.20, where a total $1.86\text{-}\mu\text{m}$ ice $\ell = 1$ nonuniformity was calculated. (The ice thicknesses at the north and south poles were $99.07\ \mu\text{m}$ and $100.93\ \mu\text{m}$, respectively.) The results of simulation recreating other capsule $\ell = 1$ nonuniformities are listed in Table 81.III.

Case 3: Temperature gradients on the inner surface of the layering sphere.

In the model for this investigation, the temperature was raised by a fixed amount on an area covering 12% of the layering sphere. The remainder of the layering sphere was held at $19.2\ \text{K}$. This simulated the effect that a localized heat load on the layering sphere has on a target. The capsule and DT ice were initially uniform $2\ \mu\text{m}$ and $100\ \mu\text{m}$ thick, respectively. The resultant effects on the ice temperature and distribution were calculated for a target centered in the layering sphere.

The presence of helium exchange gas allowed temperature perturbations on the layering sphere to transmit to the target and create an uneven heat load. Naturally, the side of the capsule closer to the heat source was warmer than the opposite side. The DT ice thinned from the warmer side and redistributed on the cooler side, until the free DT surface was isothermal. The

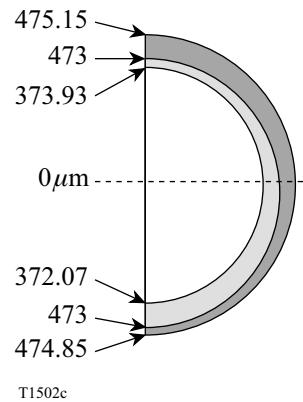


Figure 81.20
The ice’s void was shifted until zero temperature difference occurred between the poles. This was considered to be the final ice-thickness profile. Figures are not to scale.

results are listed in Table 81.IV. A 10-mK nonuniformity over 12% of the layering sphere caused a $\sim 0.5\text{-}\mu\text{m}$ ice $\ell = 1$ nonuniformity. A temperature gradient along the layering sphere greater than 10 mK must be present to change the ice thickness by a significant amount.

Summary

The temperature field within the cryogenic target is influenced by many factors, including the presence of exchange gases, target alignment within the layering sphere, target capsule thickness uniformity, temperature gradients on the layering sphere, *in-situ* target characterization methods, and external radiation. This temperature field determines the thickness uniformity of the DT-ice layer.

The temperature profile and ice $\ell = 1$ nonuniformity of the target within the OMEGA cryogenic target positioner were calculated using a thermal model in CFD simulations. The

work isolated the effect of discrete factors that affect the uniformity of the ice thickness and determined a first-order sensitivity of the ice smoothness to the effect: (1) variations in target alignment in the layering sphere, (2) capsule-thickness uniformity, and (3) temperature uniformity on the layering sphere. The resultant ice-thickness profiles were calculated for these various boundary and initial conditions.

For a target misalignment from the center of the layering sphere by 1 mm, the expected ice $\ell = 1$ nonuniformity is $\sim 1.0\ \mu\text{m}$. For a capsule $\ell = 1$ nonuniformity of $0.1\ \mu\text{m}$ in a nominal $2\text{-}\mu\text{m}$ -thick shell, the expected ice $\ell = 1$ nonuniformity is $0.6\ \mu\text{m}$. A temperature gradient along the inner surface of the layering sphere greater than 10 mK must be present to change the ice thickness more than $0.5\ \mu\text{m}$. Results from this study determine which variables have the greatest effect on the ice smoothness to guide target fabrication, layering, and cryo-engineering priorities.

Table 81.III: Pole-to-pole temperature difference before redistribution and resultant $\ell = 1$ nonuniformity for different capsule $\ell = 1$ nonuniformities.

Capsule-wall nonuniformity ($\ell = 1$) (μm)	Pole-to-pole temperature difference in ice before redistribution (μK)	Resultant ice-thickness nonuniformity ($\ell = 1$) (μm)
0.1 (1.95 to 2.05)	9.5	0.6 (99.7 to 100.3)
0.3 (1.85 to 2.15)	24.5	1.86 (99.07 to 100.93)
0.6 (1.7 to 2.3)	52.5	3.72 (98.14 to 101.86)

For an OMEGA cryo target ($2\text{-}\mu\text{m}$ capsule wall, $950\text{-}\mu\text{m}$ OD, $100\text{-}\mu\text{m}$ ice layer)

Table 81.IV: Pole-to-pole temperature difference before redistribution and resultant ice $\ell = 1$ nonuniformity for temperature gradients over 12% of the area of the layering sphere.

Temperature gradient over 12% of layer sphere area (mK)	Pole-to-pole temperature gradient in ice before redistribution (μK)	Resultant ice-thickness nonuniformity ($\ell = 1$) (μm)
5	15.4	0.34
10	28.7	0.54

ACKNOWLEDGMENT

This work was supported by the U.S. Department of Energy Office of Inertial Confinement Fusion under Cooperative Agreement No. DE-FC03-92SF19460, the University of Rochester, and the New York State Energy Research and Development Authority. The support of DOE does not constitute an endorsement by DOE of the views expressed in this article.

REFERENCES

1. J. K. Hoffer and L. R. Foreman, *Phys. Rev. Lett.* **60**, 1310 (1988).
2. A. J. Martin, R. J. Simms, and R. B. Jacobs, *J. Vac. Sci. Technol. A* **6**, 1885 (1988).
3. J. K. Hoffer and L. R. Foreman, *J. Vac. Sci. Technol. A* **7**, 1161 (1989).
4. T. R. Dittrich *et al.*, *Phys. Plasmas* **5**, 3708 (1998).
5. Laboratory for Laser Energetics LLE Review **79**, 131, NTIS document No. DOE/SF/19460-317 (1999). Copies may be obtained from the National Technical Information Service, Springfield, VA 22161.
6. Version 5.0, Fluent, Inc., Lebanon, NH.
7. P. C. Souers, *Hydrogen Properties for Fusion Energy* (University of California Press, Berkeley, 1986).
8. H. Yokoyama, *Cryogenics* **35**, 799 (1995).
9. Kapton product literature, DuPont® High Performance Polymers, Circleville, OH.
10. "NIST-Thermophysical Properties of Pure Fluids," computer code, NIST Std. Ref. Database 12 (1992).
11. F. Y. Tsai, E. L. Alfonso, S.-H. Chen, and D. R. Harding, "Mechanical Properties and Gas Permeability of Polyimide Shells Fabricated by the Vapor Deposition Method," to be published in *Fusion Technology*.
12. J. R. Welty, C. E. Wicks, and R. E. Wilson, *Fundamentals of Momentum, Heat, and Mass Transfer*, 3rd ed. (Wiley, New York, 1984), p. 247.